Article

Journal of
Nanoscience and Nanotechnology
Vol. 15, 1280–1286, 2015
www.aspbs.com/jnn

Biogenic Preparation of Gold Nanostructures Reduced from *Piper longum* Leaf Broth and Their Electrochemical Studies

K. Mallikarjuna[1], G. Narasimha[2], N. John Sushma[3], G. R. Dillip[1], B. V. Subba Reddy[4], B. Sreedhar[4], and B. Deva Prasad Raju[5,*]

[1] *Department of Physics, Sri Venkateswara University, Tirupati 517502, India*
[2] *Department of Virology, Sri Venkateswara University, Tirupati 517502, India*
[3] *Department of Biotechnology, Sri Padmavati Women's University, Tirupati 517502, India*
[4] *Natural Product Chemistry, CSIR-Indian Institute of Chemical Technology, Hyderabad 500007, India*
[5] *Department of Future Studies, Sri Venkateswara University, Tirupati 517502, India*

Exploitation of green chemical procedures for the synthesis of metal nanoparticles by biological process has received great attention in the field of nanotechnology. To demonstrate a biogenic method that involves the reduction of aqueous gold ions by the extract of *Piper longum* leaves leading to the formation of different morphological gold nanoparticles (AuNPs). The formation of gold nanostructures has been characterized by UV-Vis absorption spectroscopy. The X-ray diffraction (XRD) and selected area electron diffraction (SAED) patterns indicates the AuNPs are highly crystalline nature with the face-centered cubic (111), (200), (220) and (311) facets, respectively. The AuNPs have different sizes and morphologies that are identified by TEM studies. The involvement of water soluble bio-molecules such as carboxylic acids, flavonoids, proteins and terpenoids were identified by Fourier transform infrared (FT-IR) and Raman spectrum. The responsible mechanism of improving acidic nature and the process of encapsulation of gold nanoparticles by *Piper longum* extract was discussed. Additionally, we have demonstrated the modified carbon paste electrode using gold nanoparticles by means of cyclic voltammetry in a solution of 1 M KCl and 1 mM $[Fe(CN)_6]^{3-/4-}$. The analysis of cyclic voltammetry shows electronic transmission rate between modified Au-CPE and Bare-CPE electrode increased.

Keywords: *Piper longum* Leaves, Optical Properties, Au Nanoparticles, Green Synthesis.

1. INTRODUCTION

Green nanotechnology is an emerging field in the area of nanoscience and nanomedicine which is dedicated for the creation, improvement and utility of nanostructures for advanced material science, bio-imaging and sensors. The proliferation of green nanotechnology has sprouting the inter-disciplinary research in the diverse fields such as medicine, catalysis, drug delivery, coatings etc.[1–5] The synthesis of nanoparticles with desired shapes and sizes is a major challenging task for the emerging area of material research in green nanobiotechnology.[6,7] Gold nanostructures have attracted considerable attention due to their unusual shape dependent surface plasmon resonance and their potential application in biomedical field including cancer therapy.[8,9] As a result, a variety of green approaches have been reported for the synthesis of metal nanoparticles using various biological sources.[10–15] In addition, there are some reports on the synthesis of metallic triangular nanostructures using biomaterials.[16–18] The optical properties of nanoparticles changes slightly from visible to near IR region, when the metal nanoparticles are enlarged.[19,20] In particular, the gold triangular nanostructures hold considerable promise for biomedical and photonic applications.[21–25] A variety of gold nanostructures including rods, triangles, hexagons, octagons, cubes, disks, nanowires and nanotubes have been synthesized by physical and chemical methods.[26–31] However, most of these methods are cost-intensive and hazardous

*Author to whom correspondence should be addressed.

 1533-4880/2015/15/1280/007 doi:10.1166/jnn.2015.8889

to human health and environment.[32] In fact, Nature provides a solution in the form of biomolecules that can be successfully utilized for capping the various metal nanostructures.[33] Of various plants, herbs and spices often contain high levels of powerful antioxidants such as phytochemicals in their roots, stems, fruits and leaves which act as a natural reducing and stabilizing agents for metal nanoparticles.[8] These naturally occurring antioxidants have proved to be non-toxic to living organisms and the environment. Consequently, there is a renewed interest in green approaches for the synthesis of metallic nanoparticles through environmentally benign, biodegradable and non-toxic materials. The bio-organic moieties of *Piper longum* have various chemical constituents such as unsaturated amides, flavonoids, lignans, aristolactams, long and short chain esters, terpenes, steroids, prophenylphenols, and alkaloids are possess pharmacological properties like anti-tuberculosis, anticancer, antimalarial, antioxidant, antiamebic properties.[34–36] The *Piper longum* is a medicinal plant which is being used in Indian traditional medicine such as Ayurveda, Siddha, and Unani and in tribal/folk medicine.[37, 38] It is known to display promissing antioxidant, anti-microbial, anti-inflammatory, anti-tumor and anti-cancer activities. In the current study, we explore the ability of *Piper longum* leaf extract as reducing and stabilizing agent to produce gold nanostructures.

2. MATERIALS AND METHODS

2.1. Materials

Hydrogen tetrachloroaurate(III) trihydrate ($HAuCl_4 \cdot 3H_2O$) was obtained from Sigma-Aldrich and used without further purification. The fresh *Piper longum* leaves were collected from the Green house. The fine graphite powder, KCl, Potassium ferrocyanide was obtained from Merck chemicals. Silicon oil, acetone (GR grade) was procured from Himedia chemicals. All chemicals used are analytical grade and the aqueous solutions were prepared with double distilled water.

2.2. Preparation of *Piper longum* Leaf Extract

About 20 g of fresh leaves were thoroughly washed and then finely chopped into leaf pieces and placed in a 250 mL Erlenmeyer flask containing 100 mL of double distilled water. The resulting leaf suspension was boiled for 5 min and the extract was cooled and then filtered through the whatman no. 41 filter paper (pore size 20 μm) and stored at 4 °C for further experiments. The condensed liquid was used for the synthesis of gold nanoparticles.

2.3. Synthesis of Gold Nanoparticles

The gold nanoparticles were prepared by treating of 10 mL of 0.001 M $HAuCl_4 \cdot 3H_2O$ with aqueous extract and the mixture was kept at dark place. The visual appearance of a purple color in the reaction vessels indicates the formation of gold nanoparticles.

3. CHARACTERIZATION

The kinetics of the reaction between leaf extract and chloroauric solution was analyzed by UV-Vis absorption spectroscopy. The analysis was carried out on Thermo Scientific Genesys 10S UV-Vis spectrophotometer with samples in a 1 cm path length quartz cuvette operated at a resolution of 1 nm. The nanoparticle solution was diluted with doubled distilled water to avoid errors due to high optical density value of the solution and doubled distilled water was used as a blank. The particle size and morphology were examined with Philips Tecnai F 12 transmission electron microscope operating at an accelerating voltage 15 kV. For TEM measurements, grids were prepared by placing a drop of the bio-reduced AuNPs solution onto a carbon coated copper grid and later dried at room temperature after removing the excess solution using filter paper. For X-ray diffraction (XRD) measurements, the thin film was analyzed by a drop of AuNPs solution coated onto a glass slide, which was analyzed by using Inel C120 X-ray diffractometer, and is equipped with a curved position sensitive detector and the data was collected using Co-K_α radiation of 1.7889 Å. The IR spectrum was analyzed on Thermo-Nicolet IR 200 spectrophotometer, operated at a resolution of 4 cm^{-1} in the region of 4000–400 cm^{-1}. For this, the sample was centrifuged at 15000 rpm for 30 min and dried in air. The p^H values were measured with Elico U 120 p^H meter and a combined p^H CL 51 B electrode. The Raman spectrum was analyzed on LABRAM HR 800 micro Raman spectrometer coupled with confocal microscope. Electrochemical measurements were performed on CHI model 660c electrochemical work station with a connection to the personal computer that was used for electrochemical measurements. A conventional three electrode cell was employed throughout the experiments, with a bare carbon paste electrode (Bare-CPE) (homemade cavity of 3.0 mm diameter)/Au doped carbon paste electrode (Au-CPE) as a test electrode, saturated calomel electrode (SCE) as a reference electrode and a platinum wire as a counter electrode. The electrochemical behavior of Bare-CPE and Au-CPE electrode was studied by using cyclic voltammetry in 1 M KCl in potential range of −0.2–0.6 V at 30 mV/Sec.

3.1. Preparation of Bare and Modified Carbon Paste Electrode

The bare carbon paste electrode was prepared by hand mixing of 70% graphite powder and 30% silicon oil in an agate mortar to produce a homogenous carbon paste. The paste was packed into the cavity of homemade PVC (3 mm in diameter) and then smoothened on a weighing paper. The electrical contact was provided by copper wire connected to the paste at the end of the tube.[39] The modified carbon paste electrode was prepared by taking different volume of AuNPs (5, 10, 15 and 20 μl) in silicon oil 30% and graphite powder 70%. The prepared modified carbon paste electrode and bare electrode was packed into a

homemade Teflon cavity current collector and smoothened on a weighing paper. All the experiments were carried out at room temperature $30 \pm 2°C$.

4. RESULTS AND DISCUSSION

4.1. UV-Vis Absorption Spectroscopic Studies

The UV-Vis spectra of gold nanoparticle formation at constant concentration of $HAuCl_4$ (1 mM) with varying quantity of *Piper longum* leaf extract of 0.5 mL, 1.0 mL, 1.5 mL, and 2.0 mL aqueous medium shown in Figure 1. It is evident that a small shift of absorbance peak towards the lower wavelength region (555–546 nm) with increasing amount of the leaf extract. The gradual color change from pink to ruby red was observed during reaction with varying quantity of extract which are characteristic of the surface plasmon resonance (SPR) of AuNPs in solution. As a function of leaf extract increases, the width of the SPR peak is decreases, indicating that the synthesized AuNPs are spherical in shape. The growth of nanoparticles was recorded through the changes in UV-Vis spectra with time which are depicted in Figure 2. The intensity of absorbance peak (540 nm) of AuNPs was increases with time (up to 1 hours). After one hour, we observed two prominent differences in the absorption spectrum, one is the intensity of SPR peak which is decreased and a new absorption band is developed at 650 nm indicating the presence of anisotropic nanostructures. With increasing reaction time from 1.5 h to 2 and 3 h, the SPR band at 650 nm was shifted towards the red region (720 nm) which clearly indicates the anisotropic shape of the gold nanostructures.[40,41] The characteristic feature of anisotropic gold nanostructures such as spherical, hexagons and triangles were observed by TEM studies. The UV-Vis absorption spectra of AuNPs with variable p^H values from 2 to 8 were shown in Figure 3. From the spectra, it was noticed that with increase of p^H value, the plasmon peak appears at red shift by 5 nm and also increases the broadness of the SPR, which indicates that the nanoparticles are anisotropic and uneven distribution.

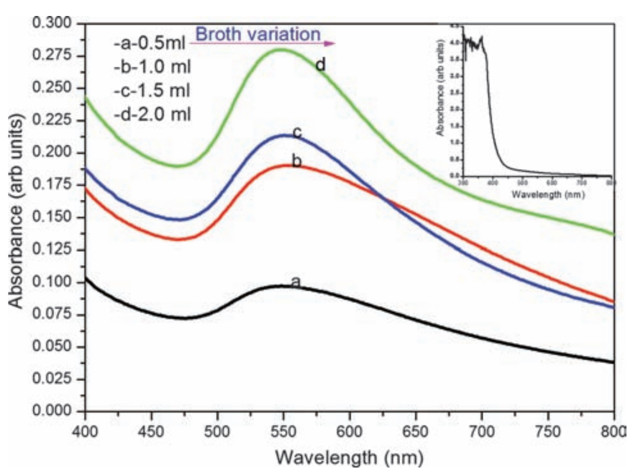

Figure 1. UV-Vis spectra of aqueous $HAuCl_4$ with *piper longum* leaf extract. Inset of the figure shows the UV-Vis spectrum of *piper longum* leaf extract.

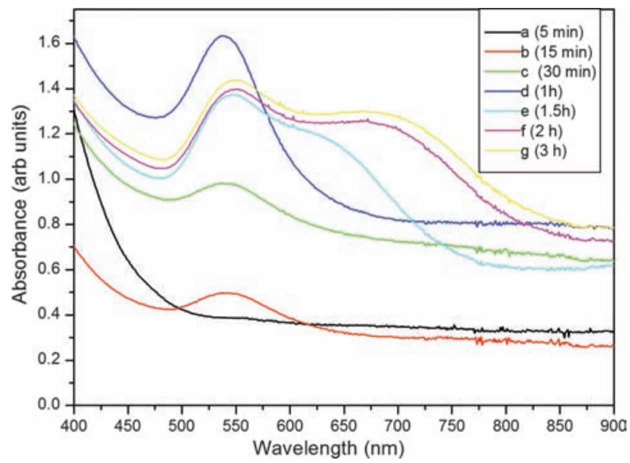

Figure 2. UV-Vis spectra of gold ions with *piper longum* leaf extract at different time intervals.

4.2. TEM, SAED and EDS Studies

The particle morphology, size, crystallinity and elemental analysis were studied from TEM, SAED studies. Figure 4 shows the TEM micrograph of the biosynthesized gold nanostructures. From the micrographs, it is interesting to note that almost all the particles are not in physical contact and are surrounded by a thin layer of biomolecules, which seems to be responsible for stabilizing the nanoparticles. The nanoparticles are in hexagons, triangles and very few of the particles are spherical shape which is consistent with the enlarged SPR band in UV-Vis spectra. The size of the grown gold nanostructures was in the order of 10–150 nm. The SAED pattern suggests that the particles are highly crystalline nature in which the diffraction rings from inner to outer, clearly indicating the fcc

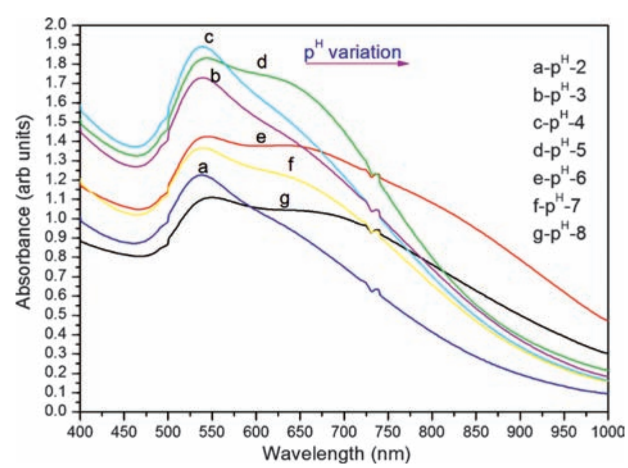

Figure 3. UV-Vis spectra of aqueous gold ions with *piper longum* leaf extract at different p^H values.

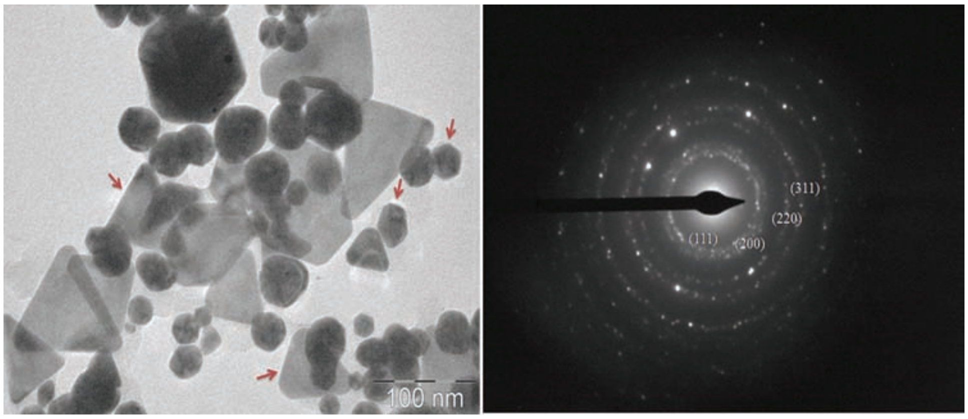

Figure 4. Transmission electron microscopy image of gold nanostructures reduced from 2.0 ml of leaf extract (arrows indicates the thin layer of biomolecules) and SAED pattern of the gold nanostructures.

facets of gold with (111), (200), (220) and (311) reflections respectively as shown in Figure 4.[42] The energy dispersive spectrum (Fig. 5) revealed the clear identification of the elemental profile of the synthesized nanoparticles, which suggests the presence of gold as the ingredient element.

4.3. XRD Analysis

The crystalline nature of the AuNPs was confirmed from XRD analysis as shown in Figure 6. A number of strong Bragg's diffracted peaks was observed at 44.6°, 52.1°, 76.8° and 93.4° corresponding to (111), (200), (220) and (311) reflections respectively. Angular positions of the diffracted Bragg peaks were compared with standard JCPDS 04-0784 file and it was confirmed that the nanoparticles have a face-centered-cubic facets respectively. The size of the gold nanoparticles are calculated by X-ray line broadening method using the Debye-Scherrer's formula $D = 0.9\lambda/\beta\cos\theta$, where D is the average size of the particle, λ is the wavelength of the incident X-rays, β is the FWHM of the diffraction peak. The calculated average domain size of the AuNPs was 23 nm using the full width half maximum (FWHM) of the (111) Bragg's reflection.[43,44]

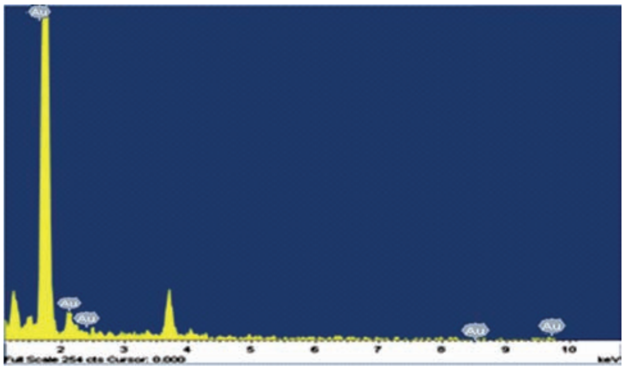

Figure 5. EDX spectrum of gold nanoparticles.

4.4. FT-IR Analysis

FT-IR has emerged as a valuable tool to understand the involvement of functional bio-organic groups in metal interactions. The FT-IR spectrum of AuNPs using *Piper longum* leaf broth is shown in Figure 7. It indicates that the functional groups present in biomolecules act as the reducing and the stabilizing agents for the formation of AuNPs. The band at 3420 cm^{-1} corresponds to N—H stretching vibrations in amides and amines and O—H stretching vibrations of hydroxyl group in alcohols and the peak at 2920 cm^{-1} indicates the C—H stretching vibration modes of hydrocarbon chains.[45] Absorption band at 2360 cm^{-1} represents the CO_2 dissolved in water.[46] The peak at 1740 cm^{-1} indicates the C=O stretching of esters and α,β-unsaturated ketones. The absorption peaks at 1640 and 1535 cm^{-1} are due to the C=C stretching and aromatic stretching vibrations, respectively. It indicates the presence of flavonoids in the leaf extract. These flavonoids may be involved in the catalytic reduction of Au^{3+} ions to Au^0 nanoparticles with interaction of carbonyl groups and glycosides which act as capping agents. The band at 1450 cm^{-1} corresponds to geminal methyl

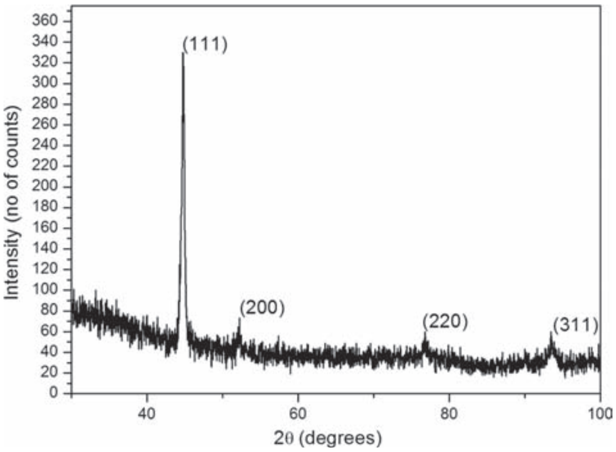

Figure 6. X-ray diffraction spectrum of gold nanoparticles.

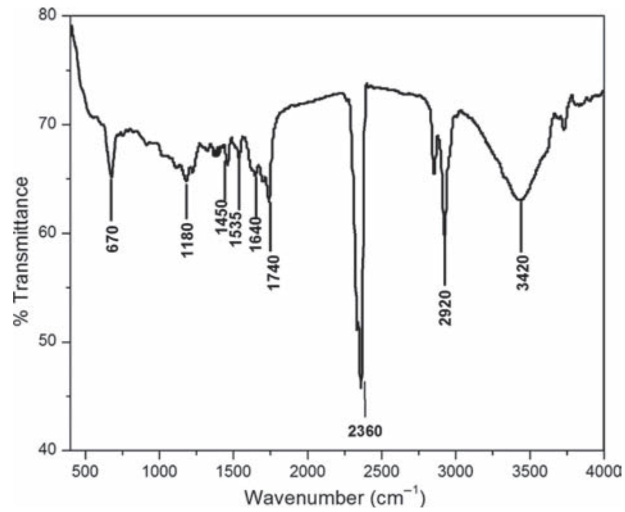

Figure 7. FT-IR spectrum of gold nanoparticles.

group stretching vibrations and peak at 1180 cm^{-1} indicates –O– vibrations.[46] The carbonyl groups from amino acid residues and peptides of proteins have a strong affinity to bind with metals; hence the proteins and glycosides are acting as encapsulating agents and protect the nanoparticles from the agglomeration. The capping agents of the biomolecules were insufficient to stabilize complete gold nuclei.[45,46] The first gold nanoparticles formed thermodynamically unstable due to their small and insufficient capping agent. The uncovered face of gold nanoparticles could oriented each other through dipole–dipole interactions of biomolecules and hydroxide ions could act as possible driving forces for the formation of anisotropic nanoparticles. In addition, the surface energy of larger particles is lower than that of smaller ones.[47,48] These small nanoparticles were suitable to dissolve in solution and grow onto larger ones. The nanoparticles grew and joined together because of their Brownian motion in the solution forming anisotropic nanostructures.[49,50] The possible pathway of the growing nanostructures by biological method is as shown in Figure 8.

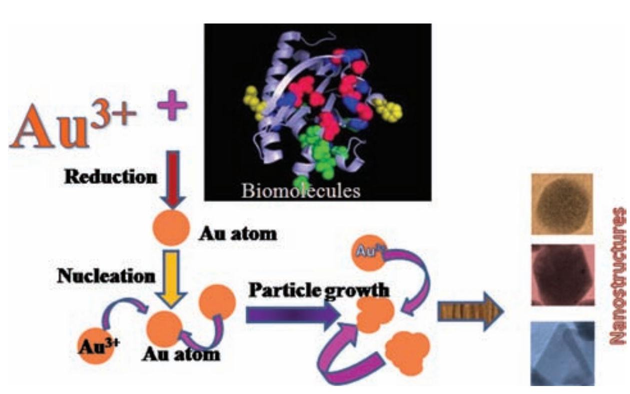

Figure 8. Mechanism for the formation of gold nanostructures with various morphologies by biological procedure.

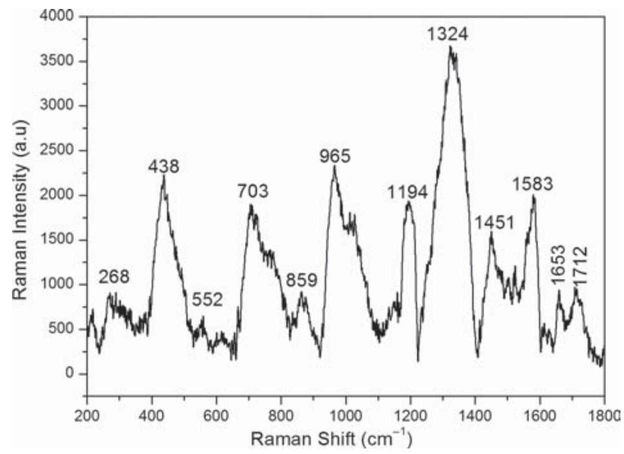

Figure 9. Raman studies of biogenic gold nanostructures.

4.5. Raman Studies

The Raman studies of biological synthesized gold nanostructures are as shown in Figure 9. The enhancement of strong peak at 438 cm^{-1} corresponds to in-plane vibrations of –C–S atoms. The weak peak at 558 cm^{-1} indicates the vibrations of —C—Cl atoms. The peak at 703 cm^{-1} corresponds to the plane vibrations of the —C—H atoms. The strong band at 965 cm^{-1} suggests the vibrations of —C—C and —C—N atoms. The enhancement of bands at 859, 1194, 1324 and 1451 cm^{-1} corresponds to the NH_2 and CH_2 twisting vibration modes which suggest the presence of interactions between positively charged secondary amino groups and negatively charged AuNPs via electrostatic interaction.[22] The enhancement of the peaks at 1653 and 1712 cm^{-1} corresponds to the amino group ($-NH_3^+$) and carboxyl group ($-COO^-$). The peak at 268 cm^{-1} suggests the stretching vibrations of Au–N atoms. The enhancements observed for all the groups suggest the presence of central carbon atom, nitrogen atom and Π-electrons of phenyl ring which behave as possible interaction sites.[51–53] Additionally, Raman spectrum is expected to be closely related to its spherical, triangular and hexagonal morphology because the edges of the particles are made of the surface roughened. The enhancement was attributed to the electromagnetic effects in aggregates combined with either molecular or metal to molecular resonances of the nanoparticles.

4.6. Hypothetical Explanation of Encapsulation and Acidic Nature of Solution

In the bio-reduction process of gold nanoparticles, the leaf extract was added to 10 mL of 0.001 M $HAuCl_4$ solution. The ionization took place as follows: It is assumed that the gold ions enter inside the plant cell passing through the H^+ ATPase protein embedded in the thylakoid membrane by an electrogenic pump. On the basis of this principle of chemistry of photography; we assume that alcoholic compound acts as a main reducing agent

Table I. p^H values of the extract in different time span.

Sample	Value of p^H
Piper longum extract (sample 1)	5.04
Aqueous solution of $HAuCl_4 \cdot 3H_2O$ (sample 2)	1.38
Sample 1 + Sample 2	
Time period (min)	
3	1.58
15	1.48
30	1.43
45	1.40
60	1.38
75	1.34
120	1.32
150	1.31

for reduction of gold ion to gold metal during the non cyclic photophosphorylation.[54] Previously, it was assumed by the researchers that the polyol components were mainly responsible for reduction of silver ions from silver nitrate. It was also reported that chlorophyll pigment might be capping the silver nanoparticles.[55] During non-cyclic photophosphorylation, many chlorophyll pigments serve as an antenna, collecting light and transferring its energy to the reaction center.[56] The stabilization of the gold nanoparticles through the H^+ ATPase protein embedding, the acidic nature of aliquot solution increases as the time increases (Table I). As shown in Table I, it was observed that the ATPase proteins act as capping agents during the process of formation of gold nanoparticles. During the above process, ATP hydrolyses to ADP liberating a phosphate group which is a source of H^+ ions. These H^+ ions may react with Cl^- ions of $HAuCl_4$ and generates HCl. Due to this reason, the acidic nature of the aliquot solution increases with time span. The anisotropic gold nanostructures are formed by the selective binding of a large number of spherical AuNPs, approaching from multiple directions to specific crystals of the initially formed small nanoparticles under limited protein concentration.[57,58]

4.7. Electrochemical Studies

The cyclic voltammetry responses of 1 mM $[Fe(CN)_6]^{3-/4-}$ in a 1 M KCl solution at the Bare-CPE and modified electrode doped with various volume of 5 μl, 10 μl, 15 μl and 20 μl of 0.001 M AuNPs were carried out at a scan rate 30 mV/sec as shown in Figure 10. The electron transfer kinetics of a redox couple in the solution on the AuNPs assembled electrodes depend on the surface of the carbon paste electrode. From the voltammetric results for the detection of Au amount on the electrode surface, we observed that a larger Au reduction signal was obtained for a higher Au amount on the electrode surface and for a higher AuNPs surface area ratio. Finally, the redox peak currents were increased gradually with increasing of AuNPs volume in the bare carbon paste and showed maximum redox current value at 20 μl.[59–63]

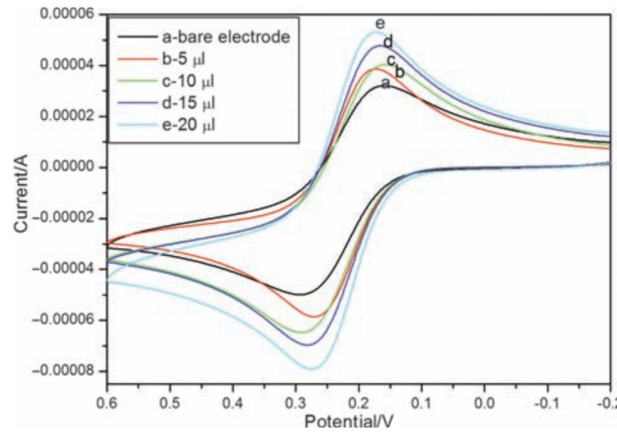

Figure 10. Cyclic voltammograms of bare and different volumes (1 mM 5, 10, 15 and 20 μl of AuNPs) of doped CPE electrodes.

5. CONCLUSIONS

In summary, we have developed a simple and convenient method for the synthesis of colloidal AuNPs and nanoplates using *Piper longum* leaf extract. By increasing the reaction time, the particle morphology of the biogenic gold was changed from spherical to nanohexagons and triangles. The crystalline nature of the nanoparticles has been studied from XRD and SAED pattern. The nanoparticles are found to be surrounded by thin layer of biomolecules. The internal conversion of polyols into carbonyl group in flavonoids may be responsible for Au^{3+} ion reduction. The cyclic voltammograms shows highly separated redox peaks for AuNPs as compared with Bare-CPE due to the electro catalytic nature of the AuNPs. This method is also preferential due to its low-hazardous to environment denoting its worth and prompt for preference in various medical, industrial and bio-imaging application.

References and Notes

1. R. A. Sperling, P. R. Gil, F. Zhang, M. Zanella, and W. J. Parak, *Chem. Soc. Rev.* 37, 1896 (**2008**).
2. Z. J. Li, J. J. Li, C. Ng, L. L. Yung, and B. Bay, *Acta Pharmacol. Sin.* 32, 983 (**2001**).
3. D. T. Thompson, *Nanotoday* 2, 40 (**2007**).
4. A. S. Thakor, J. Jokerst, C. Zavaleta, T. F. Massoud, and S. S. Gambhir, *Nano Lett.* 11, 4029 (**2011**).
5. K. K. R. Datta, B. Srinivasan, H. Balaram, and M. Eswaramoorthy, *J. Chem. Sci.* 120, 579 (**2008**).
6. A. Rai, A. Singh, A. Ahmad, and M. Sastry, *Langmuir* 22, 736 (**2006**).
7. M. A. Albrecht, C. W. Evans, and C. L. Raston, *Green Chem.* 8, 417 (**2006**).
8. Z. Zhang, J. Jia, Y. Ma, J. Weng, Y. Sun, and L. Sun, *Med. Chem. Commun.* 2, 1079 (**2011**).
9. D. Raghunandan, B. Ravishankar, G. Sharanbasava, D. B. Mahesh, V. Harsoor, M. S. Yalagatti, M. Bhagawanraju, and A. Venkataraman, *Cancer Nano* 2, 57 (**2011**).
10. K. B. Narayanan and N. Sakthivel, *Adv. Colloid. Interface Sci.* 156, 1 (**2010**).
11. C. Sreelakshmi, K. K. R. Datta, J. S. Yadav, and B. V. S. Reddy, *J. Nanosci. Nanotechnol.* 11, 6995 (**2011**).
12. J. Kou and R. S. Varma, *RSC Adv.* 2, 10283 (**2012**).

13. O. V. Kharissova, H. V. R. Dias, B. I. Kharisov, B. O. Perez, and V. M. J. Perez, *Trends. Biotech.* 31, 240 (**2013**).

14. P. Dallas, V. K. Sharma, and R. Zboril, *Adv. Colloid Interface Sci.* 166, 119 (**2011**).

15. S. M. Reddy, K. K. R. Datta, Ch. Sreelakshmi, M. Eswaramoorthy, and B. V. S. Reddy, *Nanosci. Nanotechnol. Lett.* 4, 420 (**2012**).

16. S. S. Shankar, A. Rai, B. Ankamwar, A. Singh, A. Ahmad, and M. Sastry, *Nat. Mater.* 3, 482 (**2004**).

17. V. C. Varma, S. K. Singh, R. Solanki, and S. Prakash, *Nanoscale Res. Lett.* 6, 16 (**2011**).

18. D. Raghunandan, S. Basavaraja, B. Mahesh, S. Balaji, S. Y. Manjunath, and A. Venkataraman, *Nanobiotechnol.* 5, 34 (**2009**).

19. M. Deepthy, B. Amritha, R. Archana, K. Manzoor, and S. V. Nair, *J. Biomed. Nanotech.* 8, 901 (**2012**).

20. P. Sunil, M. Ashmi, S. Ritu, O. Goldie, T. Mukeshchand, and S. Madhuri, *J. Bioscience* 7, 469 (**2013**).

21. S. Lal, L. Stephan, and N. J. Halas, *Nat. Photonics* 1, 641 (**2007**).

22. M. C. Claire, C. Jingyi, C. C. Eun, V. Lihong, and W. Younan, *Chem. Soc. Rev.* 40, 44 (**2011**).

23. M. Iosin, F. Toderas, P. Baldeck, and S. Astilean, *J. Optoelectron. Adv. Mater.* 10, 2285 (**2008**).

24. V. Kumar and S. K. Yadav, *J. Chem. Technol. Biotechnol.* 84, 151 (**2009**).

25. M. O. Montes, A. Mayoral, F. L. Deepak, J. G. Parsons, M. Jose-Yacaman, J. R. Peralta-Videa, and J. L. Gardea-Torresdey, *J. Nanopart. Res.* 13, 3113 (**2011**).

26. A. Giljohann, D. S. Seferos, W. L. Daniel, M. D. Massich, P. C. Patel, and C. A. Mirkin, *Angew. Chem. Int. Ed.* 49, 3280 (**2010**).

27. N. P. Perez, D. Baranov, S. Irsen, M. Hilgendorff, L. M. Liz-Marzan, and M. Giersig, *Langmuir* 24, 9855 (**2008**).

28. H. Kura and T. Ogawa, *J. Appl. Phys.* 107, 74310 (**2010**).

29. M. C. P. Wang and B. D. Gates, *Materalstoday* 12, 34 (**2009**).

30. J. Yao, H. Yan, and C. M. Lieber, *Nature Nanotech.* 8, 329 (**2013**).

31. K. Ariga, A. Vinu, Y. Yamauchi, Q. Ji, and J. P. Hill, *Bull. Chem. Soc. Jpn.* 85, 132 (**2012**).

32. C. N. R. Rao, H. S. S. R. Matte, V. Rakesh, and A. Govindaraj, *Dalton Trans.* 41, 5089 (**2012**).

33. K. N. Thakkar, S. S. Mhatre, and R. Y. Parikh, *Nanomedicine* 6, 257 (**2010**).

34. A. A. Amran, Z. Zakaria, F. Othman, S. Das, S. Raj, and N. M. M. Nordin, *Lipids in Health and Disease* 9, 1 (**2010**).

35. S. K. Nune, N. Chanda, R. Shukla, K. Katti, R. R. Kulkarni, S. Thilakavathy, S. Mekapothula, R. Kannan, and K. V. Katti, *J. Mater. Chem.* 19, 2912 (**2009**).

36. K. B. Narayanan and N. Sakthivel, *Adv. Colloid. Interface Sci.* 169, 59 (**2011**).

37. R. N. S. Yadav and M. Agarwala, *J. Phytology* 3, 10 (**2011**).

38. M. Zaveri, A. Khandhar, S. Patel, and A. Patel, *Int. J. Pharm. Sci. Rev. Res.* 5, 67 (**2010**).

39. K. Gangadhara Reddy, G. Madhavi, B. E. Kumara Swamy, Sathish Reddy, A. Vijaya Bhaskar Reddy, and V. Madhavi, *J. Mol. Liq.* 180, 26 (**2013**).

40. V. Bansal, A. Bharde, R. Ramanathan, and S. K. Bhargava, *Adv. Colloid Interface Sci.* 179, 150 (**2012**).

41. D. Mubarak Ali, J. Arunkumar, K. Harish Nag, K. A. S. S. Ishack, E. Baldev, D. Pandiaraj, and N. Thajuddin, *Colloids Surf. B* 103, 166 (**2013**).

42. A. K. Jha and K. Prasad, *J. Bioscience* 7, 245 (**2013**).

43. K. Mallikarjuna, G. Narasimha, G. R. Dillip, B. Praveen, B. Shreedhar, C. Sreelakshmi, B. V. S. Reddy, and B. Deva Prasad Raju, *Digest. J. Nanomat. Biostruct.* 6, 181 (**2011**).

44. R. Vijayakumar, V. Devi, K. Adavallan, and D. Saranya, *Physica E* 44, 665 (**2011**).

45. R. Deshpande, M. D. Bedre, S. Basavaraja, B. Sawle, S. Y. Manjunath, and A. Venkataraman, *Colloids Surf. B* 79, 235 (**2010**).

46. M. S. Akhtar, J. Panwar, and Y. S. Yun, *ACS Sustainable Chem. Eng.* 1, 591 (**2013**).

47. Y. Wang, L. Q. Chen, Y. F. Li, X. J. Zhao, L. Peng, and C. Z. Huang, *Nanotechnology* 21, 305601 (**2010**).

48. K. M. Kumar, B. K. Mandal, M. Sinha, and V. Krishnakumar, *Spectrochim. Acta A* 86, 490 (**2012**).

49. S. He, Y. Zhang, Z. Guo, and N. Gu, *Biotechnol. Prog.* 24, 476 (**2008**).

50. C. Laura, M. L. Blazquez, J. S. Munoz, G. Felisa, G. B. Camino, and B. Antonio, *Process Biochem.* 46, 1076 (**2011**).

51. C. Ganesh Kumar, S. K. Mamidyala, M. Narsi Reddy, and B. V. S. Reddy, *Process. Biochem.* 47, 1488 (**2012**).

52. A. Sabur, M. Havel, and Y. Gogotsi, *J. Raman Spectroscopy* 39, 61 (**2008**).

53. S. L. Smitha and K. G. Gopchandran, *Spectrochim. Acta A* 102, 114 (**2013**).

54. N. C. Maiti, M. M. Apetri, M. G. Zagorski, P. R. Carey, and V. E. Anderson, *J. Am. Chem. Soc.* 126, 2399 (**2004**).

55. G. Rajakumar and A. A. Rehman, *Res. Vet. Sci.* 93, 303 (**2012**).

56. J. Kesharwani, K. Yoon, J. Hwang, and M. Rai, *J. Bionanosci.* 3, 39 (**2009**).

57. L. Taiz and E. Zeiger, Plant Physiology, Third edn., Sinauer Associates, U.S.A. (**2006**), Chap. 6.

58. M. A. Faramarzi and A. Sadighi, *Adv. Colloid. Interface Sci.* 189, 1 (**2013**).

59. S. M. Ghoreishi, M. Behpour, and M. Khayatkashani, *Physica E* 44, 97 (**2011**).

60. R. W. Raut, A. S. M. Haroon, Y. S. Maghe, B. T. Nikam, and S. B. Kashid, *Adv. Mat. Lett.* 4, 650 (**2013**).

61. D. Du, S. Liu, J. Chen, H. Ju, H. Lian, and J. Li, *Biomaterials* 26, 6487 (**2005**).

62. A. Bonanni, M. Pumera, and Y. Miyahara, *Phys. Chem. Chem. Phys.* 13, 4980 (**2011**).

63. C. Engelbrekt, K. H. Sorensen, J. Zhang, A. C. Welinder, P. S. Jensen, and J. Ulstrup, *J. Mater. Chem.* 19, 7839 (**2009**).

Received: 12 August 2013. Accepted: 17 September 2013.